Polymer Mutual Diffusion Measurements Using Infrared ATR Spectroscopy

John G. Van Alsten* and Steven R. Lustig

Central Research and Development, Dupont Company, Experimental Station, Wilmington, Delaware 19880-0356

Received February 27, 1992; Revised Manuscript Received May 21, 1992

ABSTRACT: A technique for measuring mutual diffusion coefficients of polymers in the melt using infrared attenuated total reflectance (ATR) spectroscopy is described. This method measures the dissolution of a polymeric diffusant into a matrix of another polymer and is applicable to any diffusion couple with infrared-distinguishable bands. In situ measurements of the diffusion of various molecular weight polystyrenes and the temperature dependence of the diffusion of poly(methyl methacrylate) are presented.

Introduction

Polymer diffusion in melts governs the kinetics of polymer welding and bonding, migration and segregation in blends, and many other transport processes. It is often necessary to obtain accurate experimental measurements of these kinetics since theoretical predictions are not always possible. A host of experimental techniques have been applied to this end with reasonable success, such as forced Rayleigh scattering, field gradient spin–echo NMR, and infrared microdensitometry; these have been well reviewed by Tirrell.[1] In many circumstances, the implementation of these techniques is not practical for many polymer scientists, and in some instances the accessible range of experimental temperatures is limited as well. We have developed a nondestructive, spectroscopic technique by which diffusivities of polymeric species can be evaluated in situ using common laboratory equipment.

This experiment utilizes infrared spectroscopy in the mode of attenuated total reflectance (ATR) to track the diffusion of one polymer into another and is applicable to any polymer mixture whose components have spectroscopically distinguishable absorption bands. A diffusion couple is prepared by sandwiching a thin film of one polymeric species (the diffusant) between an ATR element and a relatively thick film of a second polymeric species (the matrix). Subsequent heating above the polymer glass transition temperature activates large-scale center of mass motion, resulting in the dissolution of the diffusant into the matrix. Since ATR spectroscopy is selective to species near the surface of the ATR element, this dissolution may be quantitatively characterized by measuring the intensity of characteristic absorbance bands of the diffusant as a function of time. A related strategy has been developed independently by Hemmelman and Brandt[2] to measure the imbibition of small-molecule liquids into films of polyethylene.

Experimental Section

The ATR method has been utilized extensively in the analysis of polymeric materials and in interfacial studies.[3] Briefly, this technique measures selectively species within a reasonably short distance from the interface between an infrared element and a contacting material. This distance is characterized by a penetration depth, λ, over which the magnitude of the penetrating electric field, the evanescent wave, of an FTIR beam diminishes by a factor of $1/e$. The penetration depth of the evanescent wave can be calculated from eq 1. Here λ_1 is the wavelength of the infrared beam in the ATR element, θ is the angle of incidence of the radiation at the polymer/element interface, and n_{21} is the ratio of the refractive index of the polymer to that of the element.[4] With typical infrared materials and polymers, the penetration depth is typically on the order of 1 μm at mid-infrared wavelengths.

$$\lambda = \frac{\lambda_1}{2\pi(\sin^2\theta - n_{21}^2)} \quad (1)$$

The evaluation of the penetration depth requires the knowledge of the optical properties of the materials utilized. Since such data for polymers in the infrared region of the spectrum are extremely limited, it is typically necessary to measure the refractive indices for the polymers. To obtain these, solution-cast films were first roughened, coated with black pigment on one side, and then mounted on a heated stage with the virgin side exposed. This stage was then installed in a variable-angle reflection accessory (Harrick Scientific Corp. Seagull, Ossining, NY), and the reflectivity of the sample (versus an aluminum mirror) measured as a function of incident angle. These data were subsequently fit to Fresnel's equation to yield the refractive indices, as illustrated in Figure 1. Data for the index of poly(methyl methacrylate) (PMMA) at 2600 cm^{-1} versus temperature are presented in Figure 2. Optical constants for the silicon ATR elements utilized were obtained from the literature.[5] At a wavenumber of 2950 cm^{-1} and with a 45° ATR element, these constants yield a penetration depth of ca. 0.25 μm.

To prepare the diffusion couple, thin (ca. 0.02–0.5 μm) films of diffusant were deposited directly onto the face of silicon ATR elements by either spin coating or dip coating from solution. This film thickness can be determined using gravimetry, profilimetry, or ellipsometry. The film free surface is then pressed against a thick (25–125 μm) film of the matrix polymer, which is prepared by solution casting. Figure 3 illustrates schematically the final diffusion couple. The diffusion couple is then clamped in a high-temperature ATR cell (Harrick Scientific), and this assembly is subsequently mounted within an infrared spectrometer (Nicolet Model 730). The practical operating temperature range of this experiment is from room temperature to ca. 400 °C.

The diffusion experiment is initiated by raising the system temperature rapidly from below the material glass transition to the experimental temperature. Data acquisition proceeds automatically via macro programs written using the spectrometer software. Single-beam spectra are ratioed to a reference of the bare element taken at the experimental temperature and then converted to absorbance units. Integrations of characteristic absorption bands were performed using spectrometer software.

Analysis

A simple, Fickian diffusion model is often appropriate for our analysis of the diffusion couple's interpenetration. We consider diffusion of the thin film of diffusant with thickness b cast on the ATR element. Mutual diffusion occurs between the bounds of the element and the free surface of the matrix system. Since we expect undetectable changes in volume on mixing, the total thickness, a, of the

0024-9297/92/2225-5069$03.00/0

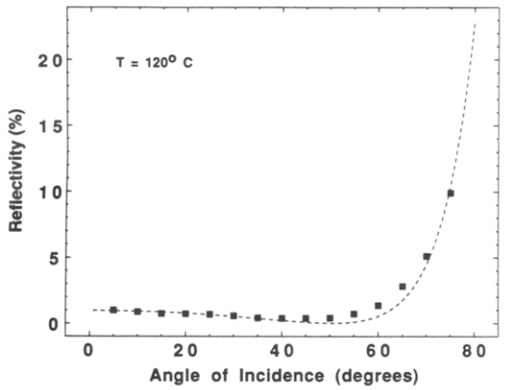

Figure 1. Reflectivity versus angle of incidence for p-polarized radiation at 3.846 μm (2600 cm^{-1}) from a PMMA film at a temperature of 120 °C. The curve represents the fit to Fresnel's equation with a refractive index of 1.21.

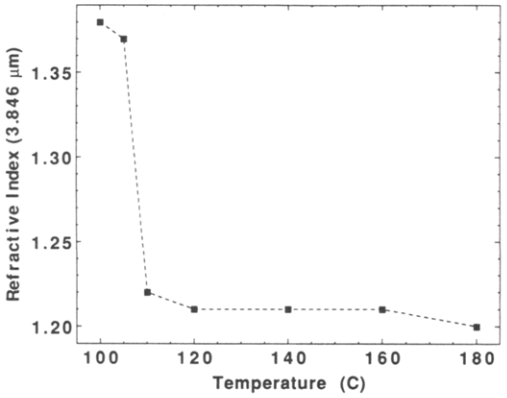

Figure 2. Temperature dependence of the refractive index of PMMA at 3.846 μm, with a large change through the glass transition.

polymer system remains constant.

$$\frac{\partial C}{\partial t} = D\frac{\partial^2 C}{\partial x^2} \qquad x \in [0,a],\ \tau \in [0,\infty] \tag{2}$$

Here $C = C(x,t)$ is the concentration of the polymer diffusant, x is position, t is time, and we assume a constant diffusion coefficient, D. Since there can be no material flux across the boundaries, we require homogeneous Neumann boundary conditions.

$$\frac{\partial C}{\partial x}(0,t) = \frac{\partial C}{\partial x}(a,t) = 0 \tag{3}$$

Initially the two polymer layers are unmixed. Hence our initial profile can be described by a step profile.

$$C(x,0) = C_0[1 - \mathcal{H}(x-b)] \qquad a > b > 0 \tag{4}$$

where C_0 is the concentration of the diffusant polymer on the ATR element and $\mathcal{H}$ is the Heaviside function. Solution of the initial/boundary-value problem defined in eq 2–4 provides the following expression for the time-dependent concentration profiles.

$$\frac{C(x,t)}{C_0} = \frac{b}{a} + \frac{2}{\pi}\sum_{n=1}^{\infty}\frac{\sin\left(n\pi\frac{b}{a}\right)}{n} \times \cos\left(n\pi\frac{x}{a}\right)\exp\left(-n^2\pi^2\frac{Dt}{a^2}\right) \tag{5}$$

The ATR technique does not measure directly concentration profiles, but an absorbance, A_t, which is proportional to the intensity of the instantaneous mass, M_t, which

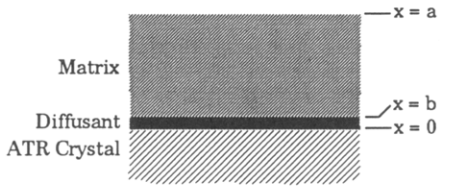

Figure 3. Illustration of the diffusion couple mounted on an ATR crystal.

is spatially weighted over the detection volume determined by the ATR penetration depth.

$$M_t = \int_0^a \alpha \exp\left(\frac{-2x}{\lambda}\right) C(x,t) S\, dx \tag{6}$$

where α is the oscillator strength, λ is the characteristic penetration depth for the evanescent FTIR beam's electric field, and S is the cross-sectional area. The experimental measurements of absorbance can be normalized between the initial absorbance value and that at infinite time. Using eqs 5 and 6, we obtain the following model for these data.

$$\frac{A_t - A_0}{A_\infty - A_0} = 1 - \frac{2}{\pi}\sum_{n=1}^{\infty}\frac{\sin\left(n\pi\frac{b}{a}\right)}{n} \times \exp\left(-n^2\pi^2\frac{Dt}{a^2}\right)\left[\frac{1 + (-1)^{n+1}\exp\left(\frac{-2a}{\lambda}\right)}{1 + \left(\frac{n\pi\lambda}{2a}\right)^2}\right] \times \left\{\left[1 - \exp\left(\frac{-2b}{\lambda}\right)\right] - \frac{b}{a}\left[1 - \exp\left(\frac{-2a}{\lambda}\right)\right]\right\}^{-1} \tag{7}$$

where A_t is the absorbance at any time, A_0 is the initial absorbance, and A_∞ is the equilibrium absorbance of the final, homogeneous system. In principle, A_∞ can be evaluated using the values of A_0, a, b, and λ, from

$$A_\infty = A_0\frac{b\left[1 - \exp\left(\frac{-2a}{\lambda}\right)\right]}{a\left[1 - \exp\left(\frac{-2b}{\lambda}\right)\right]} \tag{8}$$

In practice, we have often driven the mixing to completion by raising the temperature of the system and waited until no change in the characteristic absorptions can be discerned. The measurement of A_∞ is then taken at the reestablished experimental temperature.

At experimental temperatures near the glass transition of the diffusion couple, non-Fickian concentration profiles can exist and propagate such that the normalized absorbance can still be fit to the Fickian model in eq 7. Hence, correct interpretation of the data using eq 7 requires that the experimental system be well above the glass transition temperature for the compositions of interest.

Our analyses make the approximation of constant λ, which is technically incorrect for a system whose compositon is changing with time and depth. However, this is not a strong approximation for two reasons. First, the diffusion layer can be so small, $b < \lambda < a$, that the penetration depth is dominated by the properties of the thick film. Second, for most diffusion couples of interest, the difference in the material's refractive indices are reasonably small and lead to even smaller perturbations on λ. For example, a difference of 13% in the refractive index of poly(methyl methacrylate) versus polystyrene leads to only a 6% difference in λ with a silicon element

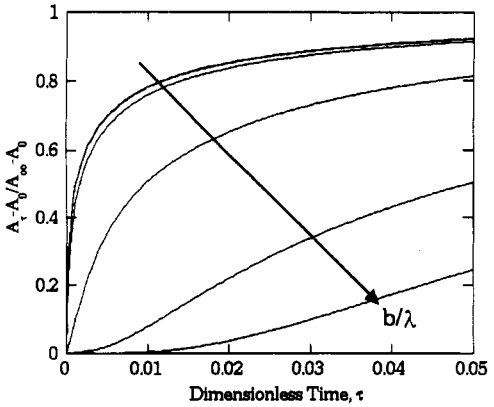

Figure 4. Calculated normalized uptake as a function of $\tau = Dt/a^2$ according to eq 7 for $a/\lambda = 10$ where $b/\lambda = 10^{-3}$ (left), 10^{-2}, 10^{-1}, 1, 3, 5, and 10 (right). Curves for b/λ less than unity are visually indistinguishable.

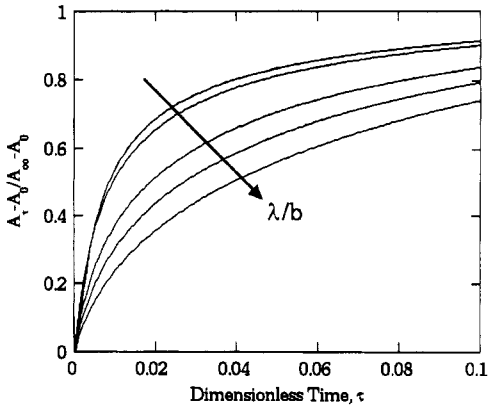

Figure 5. Calculated normalized uptake as a function of $\tau = Dt/a^2$ according to eq 7 for $a/b = 10$ where $\lambda/b = 10^{-3}$ (left), 10^{-2}, 10^{-1}, 1, 3, 5, and 10 (right). Curves for λ/b less than unity are visually indistinguishable.

at 45°. In test cases, this leads to a roughly 4% difference in the value of the fitted diffusion coefficient. This discrepancy constitutes only a minor variation by any sense given the current state of the art. For diffusion couples whose penetration depth is highly dependent on composition, the normalized absorbance can be obtained numerically by integrating eqs 5 and 6.

The experimental technique can provide mutual diffusion coefficient values over a range of compositions, depending on the relative values of a, b, and λ. We have specified $a > b$ by convention. The penetration depth of the evanescent wave defines the effective detection volume. Clearly, this experiment is only practical when $a > \lambda/2$ so that the average composition within the detection volume changes during the experiment. Consider the following three regimes defined by the relative values of a, b, and λ.

Regime I: $a > \lambda \gg b$. Here the diffusant initially occupies only a small fraction of the total sampling volume. Sampling within the evanescent wave detects the loss of the diffusant over a mean concentration $2b/\lambda$. If we construct an experiment such that $2b/\lambda$ is less than ca 10^{-3}, then we will measure a limiting diffusivity of very dilute diffusant in the concentrated matrix layer. Figure 4 illustrates solutions of eq 7 for various values of b/λ. The reader should note that the dimensionless time scale for the measurement period is considerably reduced relative to normal gravimetric experiments which equilibrate on dimensionless time scales of order unity. Hence this technique makes the measurements of very small diffusivities over macroscopic length scales more time efficient. In this case, diffusion coefficients as small as 10^{-15} cm^2/s can be measured. Although very thin layers of diffusant are stipulated in this regime, the measurements are sensibly independent of the actual value of b/λ when this ratio is much less than unity. This is illustrated in Figure 4 since curves pertaining to small values of b/λ are visually indistinguishable. In this case, accurate experimental measurements of only a and λ are required since the uptake equation, eq 7, becomes independent of the value of b/λ as the value b/λ is diminished.

Regime II: $a > b \approx \lambda$ **or** $a \approx \lambda > b$. Here we measure the mutual diffusion coefficient of the diffusant in the matrix over mean diffusant compositions of order b/a. Accurate determinations of a, b, and λ are required.

Regime III: $a > b \gg \lambda$. Here sampling within the evanescent wave volume occurs much closer to the ATR element interface than the initial diffusant/matrix interface. The diffusant is monitored over compositions spanning between its pure concentration and a dilution of b/a. Figure 5 illustrates solutions of eq 7 for various values of λ/b. The measurements are sensibly independent of the evanescent wave penetration depth when the value of λ/b is much less than unity. This is illustrated in Figure 5 in that curves pertaining to small values of λ/b are visually indistinguishable. Here accurate determinations of only a and b are required. If b/a is just less than unity, then we might consider the top, thin layer as the diffusant and the bottom thick layer as the matrix. In this case, we monitor the very dilute diffusant's arrival at the ATR element. We have found this regime is quite useful for diffusion couples with relatively high diffusion coefficients. Diffusion coefficients on the order of 10^{-4} cm^2/s can be measured in this way.

The measurements described in the following experiments are best described by regimes I and II.

An analysis of nonsystematic errors is always recommended. First, a diffusion coefficient value is obtained by minimizing the summed squared error between eq 7 to experimental data. While this step can be done nongraphically, it is recommended to access visually the fit of eq 7 to experimental data, checking for systematic, non-Fickian character in the data and instrumental artifacts. The uncertainty in the diffusion coefficient can be established by determining the propagation of probable errors. Suppose there are N number of data points of normalized absorbance, f_i, recorded as a function of time, preferably a dozen or so below 80% fractional absorbance. The uncertainty in the diffusion coefficient obtained by fitting eq 7 to time-dependent data is given in eq 9.

$$(\Delta D)^2 = \sum_{i=1}^{N}\left[(f-f_i)^2 - \left(\frac{\partial f}{\partial a}\right)_i^2(\Delta a)^2 - \left(\frac{\partial f}{\partial b}\right)_i^2(\Delta b)^2 - \left(\frac{\partial f}{\partial \lambda}\right)_i^2(\Delta\lambda)^2 - \frac{4(1-f_i^2)}{(A_\infty - A_0)^2}(\Delta A)^2\right] \Big/ \sum_{i=1}^{N}\left(\frac{\partial f}{\partial D}\right)_i^2 \quad (9)$$

The uncertainty in the diffusion coefficient, ΔD, depends on the uncertainties in the total thickness of the diffusion couple (Δa), initial diffusant thickness (Δb), evanescent wave penetration depth ($\Delta\lambda$), and integration of the absorbance peak detected in the infrared spectrum (ΔA). Here $f = f(a,b,\lambda,D,t_i)$ is the normalized absorbance function computed using eq 7 at the time of the ith datum. We typically find the uncertainty in the diffusion coefficient is 10% or less. Often the precision is limited by the uncertainty in the evanescent wave penetration depth.

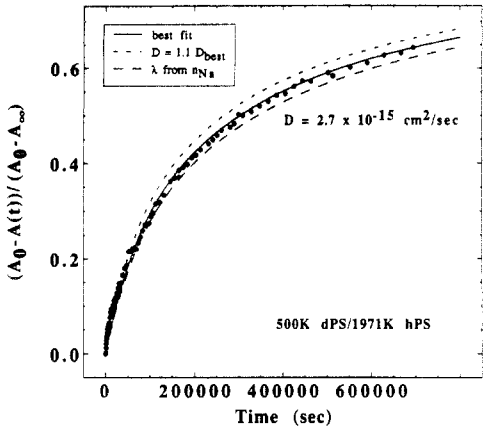

Figure 6. Experimental data for the diffusion of a 500 000 M_w deuterated polystyrene into 1 971 000 M_w hydrogenated polystyrene at a temperature of 170 °C. From the top, the curves represent the calculated uptakes from eq 7 using (a) a diffusion coefficient 10% larger than the best fit value, (b) the best fit value of 2.7×10^{-15} cm^2/s, and (c) the uptake calculated using the actual diffusion coefficient but with a λ evaluated using the polystyrene refractive index at 0.5893 μm, n_D.

Table I
Diffusion Coefficients of 104 000 M_w dPS at 170 °C

matrix M_w	D (cm^2/s)	matrix M_w	D (cm^2/s)
27 500	9.7×10^{-13}	156 000	1.5×10^{-13}
66 000	4.0×10^{-13}		

Results and Discussion

A typical result from this technique is presented as Figure 6, which illustrates uptake data for a 500 000 M_w deuterated polystyrene (M_w/M_n = 1.07) diffusing into a matrix of 1 971 000 M_w (M_w/M_n = 1.26) hydrogenated polystyrene. This figure also includes the best fit to these data generated using a diffusion coefficient of 2.7×10^{-15} cm^2/s, as well as curves which represent a 10% deviation of the diffusion coefficient from the best fit value and a fit using the best fit value but with a λ evaluated from the refractive index of polystyrene at 5893 Å, as one would find in a typical literature source.[6] The best fit is clearly excellent and obviously good to well within 10%. The use of a visible-wavelength refractive index is also seen to introduce some error but can clearly be used to give estimates of the mutual diffusion coefficient which are quite reasonable.

To test this technique, we set out to duplicate the results from the classic ion beam experiments of Green et al. for the interdiffusion of atactic polystyrenes.[7] Table I reports the results of the diffusion of a 104 000 M_w deuterated polystyrene into matrices of various molecular weight hydrogenated polystyrenes at 170 °C. The diffusion coefficients obtained are always approximately 10 times lower than those reported by Green et al. We have also measured an activation energy for diffusion of this polymer into 1 971 000 M_w hydrogenated polystyrene (Figure 7) and find that the value of 58.7 kcal/mol is in excellent agreement with the 59.9 kcal/mol reported over the same temperature regime in the secondary ion mass spectrometry (SIMS) study of Whitlow and Wool.[8] One marked disadvantage of the ATR technique versus ion beam or SIMS experiments is that it does not measure directly a concentration profile. However, in this case there is no reason to believe that the diffusion is non-Fickian and therefore not well described by the mathematical model. A strong advantage of the ATR technique is the very high quality (due to easily obtainable high signal to noise ratios with even very thin films) and quantity of data which can

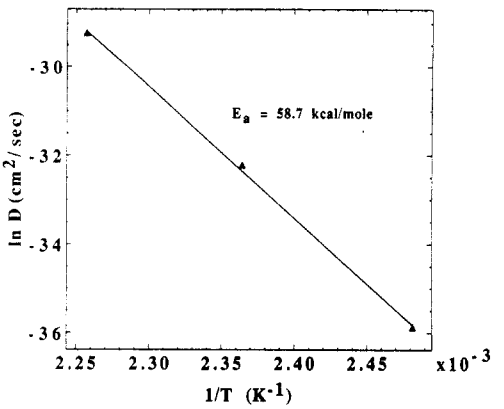

Figure 7. Activation plot for the diffusion of 104 000 M_w deuterated polystyrene into a matrix of 1 971 000 M_w hydrogenated polystyrene.

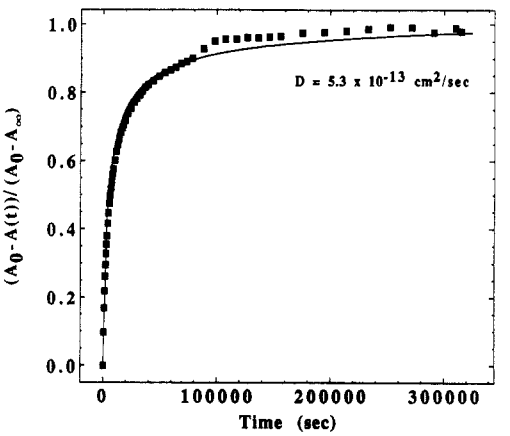

Figure 8. Experimental data for the diffusion of a 146 000 M_w deuterated PMMA into 88 000 M_w hydrogenated PMMA at a temperature of 180 °C. The curve represents the fit of eq 7 to the data with a diffusion coefficient of 5.3×10^{-13} cm^2/s.

Table II
Diffusion Coefficients of 146 000 M_w dPMMA in 88 000 M_w hPMMA

temp (°C)	D (cm^2/s)	temp (°C)	D (cm^2/s)
140	2.0×10^{-15}	180	5.3×10^{-13}
160	1.1×10^{-14}		

be acquired over the reasonably lengthy experimental times required. The profiling experiments involve annealing times on the order of 10^2–10^3 s, with the diffusivity calculated by fitting a "snapshot" of the evolving compositional profile. In contrast, the ATR experiment is typically run from 10^5–10^6 s, with the diffusivity calculated by fitting the complete temporal range. This long time frame also drastically decreases the influence of possible artifacts such as the orientation of the films from the solution-casting process,[9] residual solvent,[10] and the finite time required for molecular-scale interface formation.[11] Work is continuing in an effort to elucidate fully the discrepancies between these techniques.

To illustrate further the use of this technique and to support other research efforts, we have obtained the temperature dependence of the diffusion coefficient of atactic 146 000 M_w (M_w/M_n = 1.04) deuterated PMMA in atactic 88 000 M_w (M_w/M_n = 1.04) hydrogenated PMMA. Figure 8 illustrates typical data and the fit to the Fickian model, with the results summarized in Table II. These data yield a reasonable activation energy for diffusion of 26 kcal/mol.

Conclusions

A method for the measurement of polymer diffusion coefficients using common, commercially-available infrared equipment has been described. The technique is applicable to any diffusion couple with infrared-distinguishable bands and has been utilized here to measure the diffusivity of various molecular weight polystyrenes and to determine the activation energy for diffusion of PMMA.

References and Notes

(1) Tirrell, M. *Rubber Chem. Technol.* **1984**, *57*, 523.
(2) Hemmelman, V. K.; Brandt, H. *Exp. Tech. Phys.* **1989**, *37*, 495.
(3) See, for example: Mirabella, F. M. *J. Polym. Sci., Polym. Phys. Ed.* **1984**, *22*, 1283; Mirabella, F. M. *J. Polym. Sci., Polym. Phys. Ed.* **1984**, *22*, 1293; Yuan, P.; Sung, C. S. P. *Macromolecules* **1991**, *24*, 6095.
(4) Harrick, N. J. *Internal Reflection Spectroscopy*; John Wiley & Sons: New York, 1967.
(5) Salzberg, C. D. *J. Opt. Soc. Am.* **1957**, *47*, 244.
(6) Green, P. F.; Mills, P. J.; Palmstrom, J., Mayer, J. W.; Kramer, E. J. *Phys. Rev. Lett.* **1984**, *53*, 2145.
(7) Brandrup, J.; Immergut, E. H. *Polymer Handbook*; John Wiley & Sons: New York, 1989.
(8) Whitlow, S. J.; Wool, R. P. *Macromolecules* **1991**, *24*, 5926.
(9) Prest, W. M.; Luca, D. J. *J. Appl. Phys.* **1980**, *51*, 5170.
(10) Fernandez, M. L.; Higgins, J. S.; Penfold, J.; Shackelton, C. S. *Polym. Commun.* **1990**, *31*, 124.
(11) Yuan, B. L.; Wool, R. P. *Polym. Eng. Sci.* **1990**, *30*, 1454.

Registry No. PS (homopolymer), 9003-53-6; PMMA (homopolymer), 9011-14-7.